applied optics

Backscattering measurements of micron-sized spherical particles

Brendan M. Heffernan, Yuli W. Heinson, Justin B. Maughan, Amitabha Chakrabarti, and Christopher M. Sorensen*

Physics Department, Kansas State University, Manhattan, Kansas 66506, USA
**Corresponding author: sor@phys.ksu.edu*

Received 12 January 2016; revised 16 March 2016; accepted 21 March 2016; posted 22 March 2016 (Doc. ID 257368); published 14 April 2016

An apparatus was designed and assembled to measure scattered light in the range of 180° ± 6° where enhanced backscattering, the cause of a glory, occurs. The apparatus was calibrated and tested using Fraunhofer circular aperture diffraction, angle of incidence correction, and a diffuse reflector. Theory indicates that backscattering is strongly dependent on particle size, refractive index, and shape. Experimental measurements from polystyrene latex spheres of two sizes and water droplets showed good agreement with Mie theory, but also indicated the extreme sensitivity of the backscattering to particle parameters. The results presented should have use in the fields of particle scattering, particle metrology, and LIDAR.

OCIS codes: (290.1350) Backscattering; (220.4830) Systems design; (010.1100) Aerosol detection; (290.4020) Mie theory.

http://dx.doi.org/10.1364/AO.55.003214

1. INTRODUCTION

The glory is a beautiful pattern of concentric, colored rings occurring in nature with clouds of mist in the anti-solar direction often seen around shadows [1]. The diameters of the water droplets in the mist are typically in the 10 to 100 μm range. Whereas enhanced backscattering, which is the source of the glory, is predicted by the Mie equations, gleaning a simple physical explanation has attracted worthwhile attention [2–6]. On the other hand, there seems to be a paucity of experimental studies of backscattering. Furthermore, the work that does exist considers polarization aspects of the scattered light and is not specifically directed at the scattering intensity versus the scattering angle. Fahlen and Bryant [7,8] studied backscattering of light by water droplets ranging in diameter from 0.6 to 1.5 mm as the droplets evaporated. The droplets were either supported on thinner glass rods or acoustically levitated. They observed large, periodic intensity fluctuations that occurred with very small changes in the size parameter, which was the main objective of their work. Mie theory was successful in describing the periodicity but only semi-quantitatively successful with the scattered intensity magnitude. However, there was a concern that the droplets were distorted by gravity away from spherical. Saunders [9] used submicroscopic spider threads to support water droplets ranging from 9 to 60 μm in diameter to study backscattering. Intensity polarization ratios near 180° agreed with the theories of van de Hulst [2] and Nussenzveig [3] to within 22%. Sassen [10] studied backscattering polarization ratios from near-spherical water, ice, and mixed phase droplets in the few-millimeter-size range. He concluded that shape and homogeneity distortions significantly affect the backscattered polarization. Finally, Redding *et al.* [11] studied polarization intensity ratios for particles with irregular shapes. However, for calibration, their work included scattered intensity measurements as a function of the scattering angle in the 155°–177° range for aerosolized 3-μm-diameter polystyrene latex (PSL) spheres. These measurements agreed with Mie theory well for the parallel polarization but imperfectly for the perpendicular polarization.

Our purpose in this paper is to study the angular dependence of backscattering from spheres in the few-micron-size range. This purpose evolved from an initial goal to study backscattering from irregularly shaped particles. In that effort, we chose to calibrate our apparatus with backscattering from colloids of PSL spheres. This calibration proved to be problematic in that the measured backscattering from the purportedly well characterized PSL colloids showed variations from Mie theory. Thus, the unexpected problem arose of how well the measured backscattering from "realistic" spherical particles, i.e., those with minor uncertainties in size, refractive index, and sphericity, agrees with theory. The preceding review, which illustrates imperfect agreements between Mie theory and experiment, augments this problem.

2. EXPERIMENTAL METHODS

Figure 1 shows a schematic diagram of the light scattering arrangement for backscattering measurement. The incident laser beam with a wavelength λ of 532 nm was either vertically or horizontally polarized by placing the fast axis of the half-wave

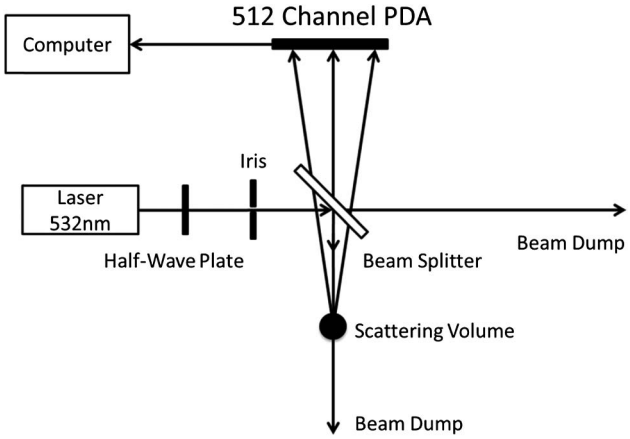

Fig. 1. Schematic diagram of the light scattering arrangement for backscattering measurements.

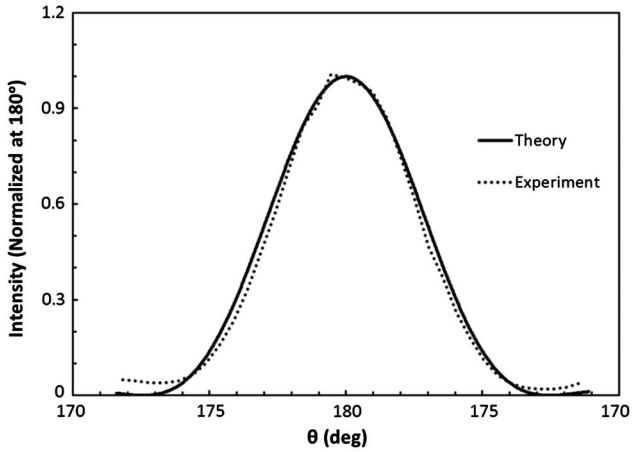

Fig. 2. Circular aperture diffraction calibration using a 5 μm-diameter pinhole. Intensity is normalized at 180°; 180° on the PDA detector corresponds to 0° for the diffraction.

plate vertically or 45° from the initially vertically polarized light of the laser. An iris was placed before the beam reaches a broadband beam splitter in order to reduce the background. The incident beam was at 45° relative to the beam splitter. Next, the reflected beam was scattered by an ensemble of particles in the scattering volume, and the scattered light transmitted through the beam splitter was detected by a 512 channel photodiode array [(PDA) Hamamatu's S3902-512]. The apparatus detected light in the range of 180° ± 6°. This sacrificed scattering in the 168°–174° range. The sacrifice was done because collecting the scattering with the exact backward direction in the center of the detectable range provided a good check for the data since they should be symmetric about 180°.

3. CALIBRATION AND TESTS

The apparatus was calibrated and tested in a number of ways:

A. Fraunhofer Circular Aperture Diffraction

To calibrate the scattering angles and intensity response, the beam splitter was removed, the laser in Fig. 1 was moved 90° counterclockwise to shine through the scattering volume, and a 5 μm-diameter circular aperture pinhole was placed at the scattering volume. Figure 2 shows our experimental data are in excellent agreement with the Fraunhofer circular aperture diffraction theory except for some minor background for $\theta < 174°$.

B. Angle of Incidence Correction

When the backscattered light from the scattering volume passed through the beam splitter, the angle of incidence (AOI) with respect to the beam splitter had a range of 45° ± 8°. The transmission of the beam splitter had a function with respect to the AOI, which needed to be measured and used for data correction.

The AOI correction was measured by placing the laser and half-wave plate so that light could pass through the scattering volume toward the beam splitter (similar to the circular aperture calibration). Next, the beam splitter was rotated through the incident angles of 45° ± 8° while the transmitted intensity was measured with either the PDA detector or a power meter, for both vertically and horizontally polarized light. To verify the method for AOI correction, the beam splitter was replaced with a piece of glass and the transmission through the glass over 45° ± 8° was measured. The results for the glass were compared to the Fresnel equations for transmittance with very good results.

C. Diffuse Reflector

A diffuse reflector (Thorlabs' DG10-1500-P01) was used to test the backscattering detection, as drawn in Fig. 1. The diffuse reflector was placed at the scattering volume. In Fig. 3, the measured scattering under the AOI correction (solid lines) is in excellent agreement (±5%) with the specifications supplied by the manufacturer shown in the dashed lines for both vertically and horizontally polarized incident light. Here and throughout, I_{vu} and I_{hu} are intensities for vertically incident and horizontally incident light, respectively, with no polarizer on the detector. In

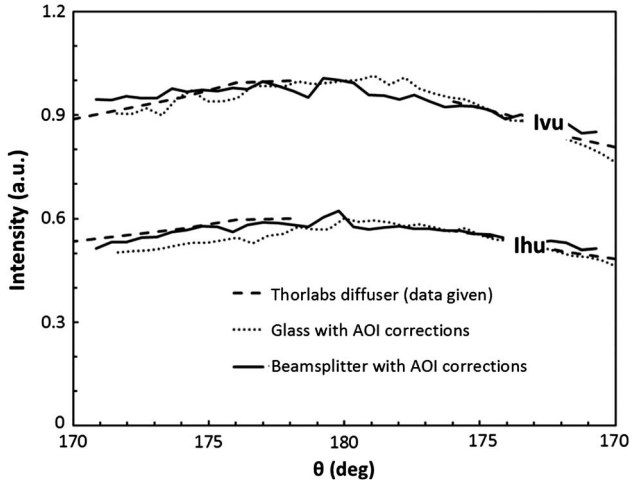

Fig. 3. Backscattering from a diffuse reflector (Thorlabs' DG10-1500-P01) under the AOI correction. The measured scattering results are shown with solid lines, and the specifications from Thorlabs are shown with dashed lines. Experimental data for the piece of glass after the AOI correction are shown with the dotted lines.

Section 3.B, we mentioned that we verified the AOI correction method using a piece of glass. Figure 3 also includes the experimental data for the piece of glass after the AOI correction (dotted lines), which is in agreement with the beam splitter although the coatings of the two are different.

4. BACKSCATTERING SENSITIVITY

In anticipation of our experimental results, we now demonstrate the large sensitivity the backscattered intensity has on the various parameters that determine the scattering by a sphere. We used the Mie theory to explore the sensitivity at a wavelength λ of 532 nm. We found that backscattering is strongly dependent on particle size, refractive index, and shape. Because the sensitivity appears to be greatest at 180° and the sensitivity at ~178° is relatively less, when we graph intensities, they will be normalized at 178°.

A. Size

Figure 4(a) shows I(180°)/I(178°) versus the radius over the range of 3–3.2 μm for a refractive index of 1.59 in a medium of 1.33 refractive index. The data were generated using Laven MiePlot [12]. Similarly, Fig. 4(b) shows I(180°)/I(178°) versus the radius over the range of 5–5.2 μm with other conditions the same. These sizes correspond to the experimental data to be described next. Large order of magnitude spikes indicate the backscattering is strongly dependent on particle size for both vertically and horizontally polarized incident light.

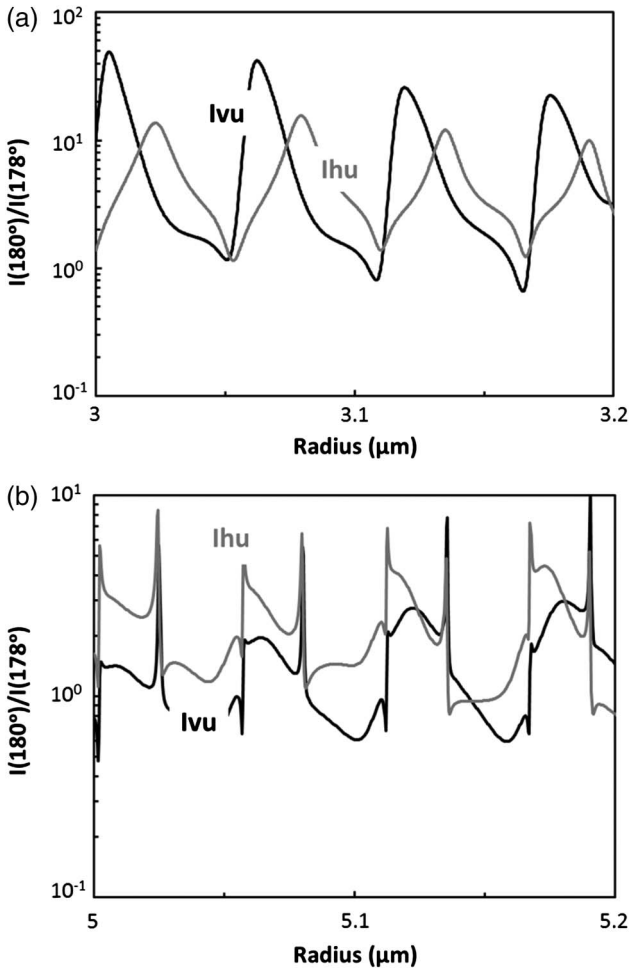

Fig. 4. (a) I(180°)/I(178°) versus radius over the range of 3–3.2 μm, (b) I(180°)/I(178°) versus radius over the range of 5–5.2 μm.

B. Refractive Index

Figure 5 shows I(180°)/I(178°) versus refractive index over the range of 1.57–1.60 for spheres with a radius of 5.055 μm in a medium with a 1.33 refractive index, e.g., water. As for the size dependence, large changes in the intensity ratio occur (factors of 1.5 to as much as 4), with small changes in the independent variable (refractive index changes of 0.002) indicating that backscattering is very sensitive to the refractive index.

C. Shape

Figure 6 presents a comparison between an ensemble of spheres (Mie) with an averaged radius of 1.4 μm (40% log-normal size distribution) and a refractive index of 1.33 and an ensemble of Gaussian random spheres (GRSs) [13] with the same specifications. However, the GRSs have 2.5% fluctuations (relative standard deviation) in the radial direction. The scattering for the GRSs was calculated using a discrete dipole approximation method [14,15]. This size and refractive index combination was chosen close to that of water droplets from prior work [16] and could not be extended to the larger sizes above due to time constraints on computation. The intensity is normalized at 178°. Figure 6 demonstrates that the backscattering is very sensitive, with changes ranging from 10% to nearly a factor of two depending on angle, to small (2.5%) deviations from the spherical shape.

We conclude that backscattering by spheres is very sensitive to size, refractive index, and shape.

5. BACKSCATTERING MEASUREMENTS FROM PSL SPHERES AND WATER DROPLETS

A. Backscattering from PSL Spheres

Two sizes of PSL sphere suspensions in water were purchased from Bangs Laboratories. The averaged radii specified by the

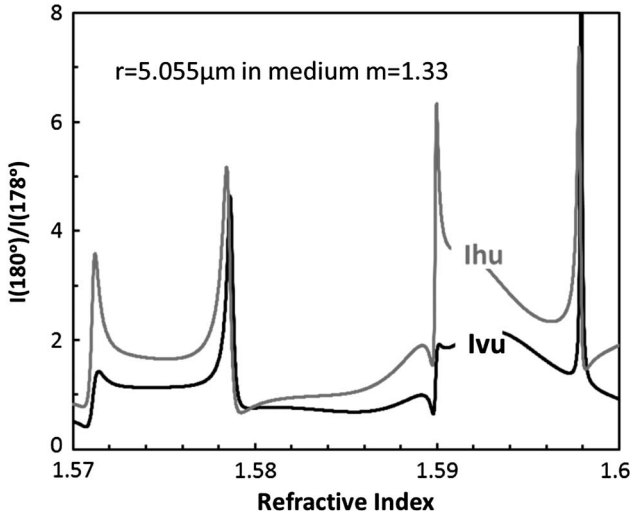

Fig. 5. I(180°)/I(178°) versus refractive index over the range of 1.57 to 1.6 for radius of 5.055 μm in a medium with a 1.33 refractive index.

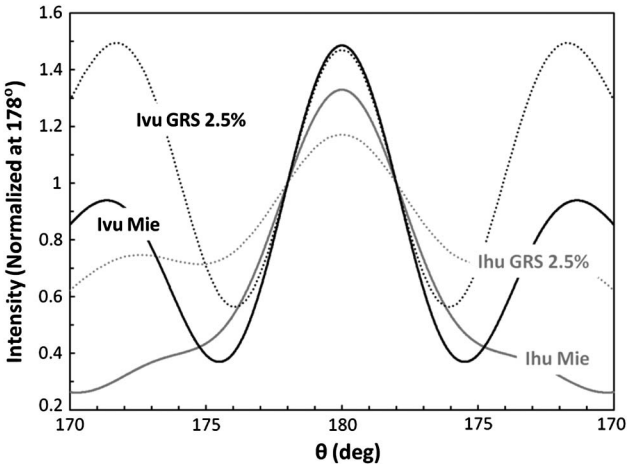

Fig. 6. Comparison between a log-normal distribution of spheres (Mie) with an averaged radius of 1.4 μm and geometric width of 1.5 and an ensemble of Gaussian random spheres (GRS) with 2.5% for the relative standard deviation in the radial direction.

manufacturer were 3.075 and 5.055 μm with a geometric size distribution width of 5% and refractive index of 1.59. A spectroscopic grade cuvette with a path length of 2 mm containing the suspensions was placed in the scattering volume. This was aligned so that the backreflection from the glass wall of the cuvette retraced the path of the laser back through the iris to the laser. It was then tipped vertically ~20° so that this reflection didn't interfere with the backscattering to the detector. Backscattered light from the colloid did not follow this wall backreflection but rather proceeded back along the incident laser beam, the 180° direction, and at other angles to each side of 180° through the beam splitter to the detector. A consistent background measurement consisted simply of either removing the cuvette or waiting for the colloid to settle. The AOI correction was applied.

Figures 7 and 8 show the backscattered intensity (normalized at 178°) versus θ for both vertical and horizontal incident polarizations for PSL spheres with average radii of 3.075 and 5.055 μm, respectively, in water. The data are compared to possible PSL refractive indices; 1.59 is the refractive index claimed by Bangs Laboratories and shown in solid lines.

The fits of the data to Mie theory for the PSL spheres is fair to good. For $R = 3.075$ μm, Fig. 7(a) shows a good fit for horizontal polarization with a refractive index of 1.580, not the

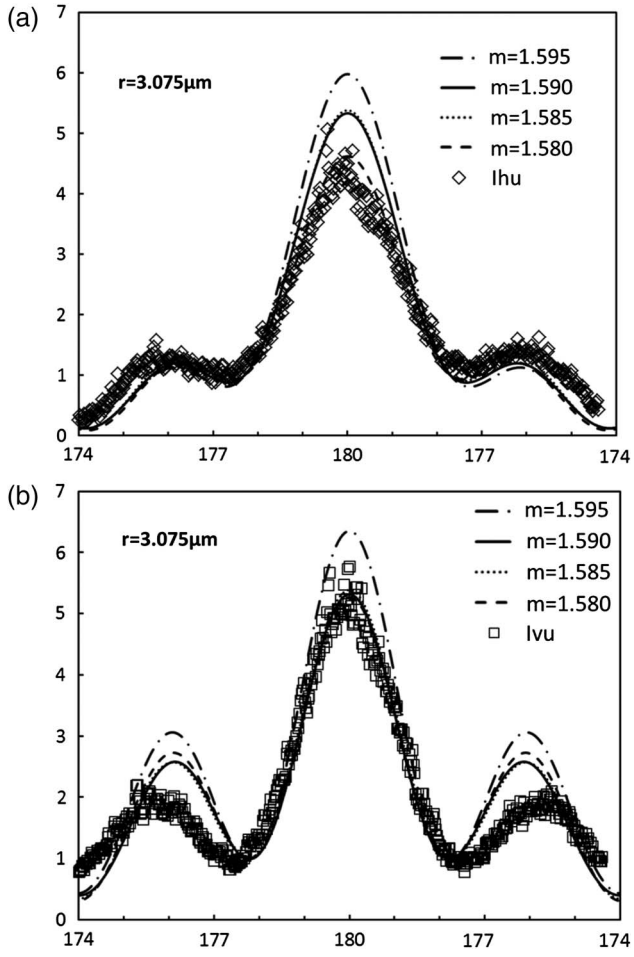

Fig. 7. Backscattered intensity (normalized at 178°) versus θ for PSL spheres with average radius of 3.075 μm; (a) horizontal polarization, (b) vertical polarization.

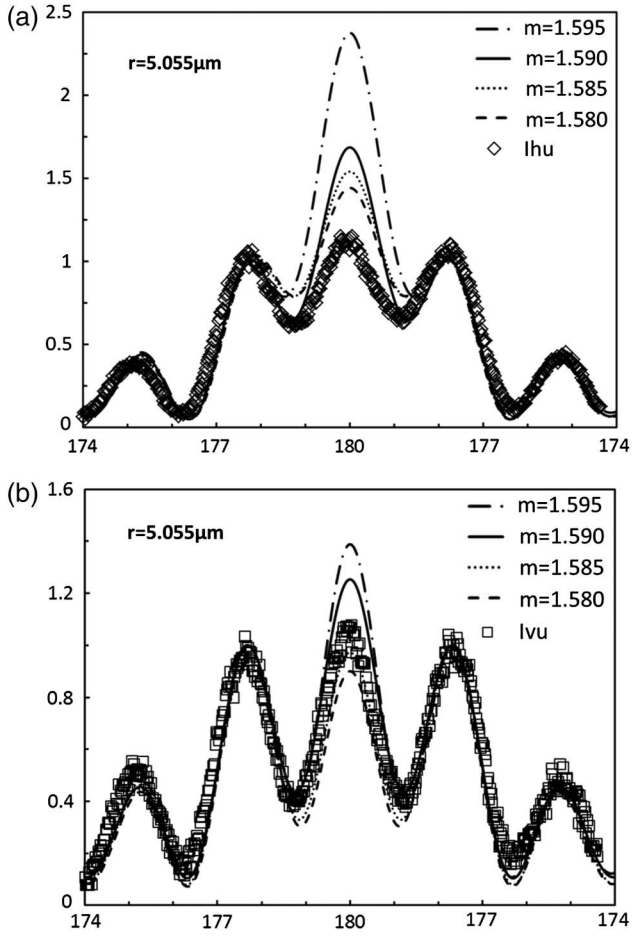

Fig. 8. Backscattered intensity (normalized at 178°) versus θ for PSL spheres with average radius of 5.055 μm; (a) horizontal polarization, (b) vertical polarization.

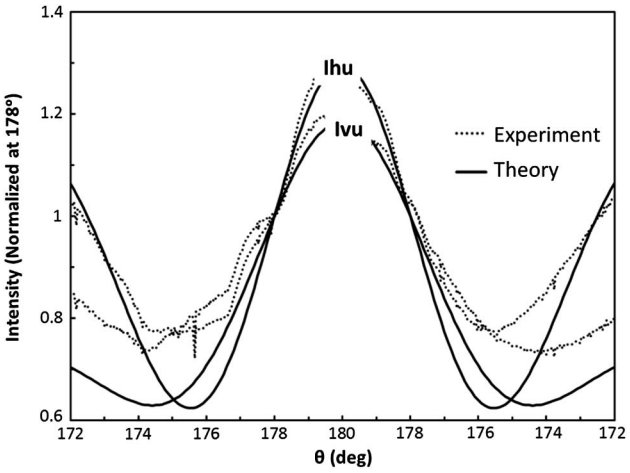

Fig. 9. Backscattering from water droplets where the intensity is normalized at 178°.

specified 1.59. Figure 7(b) for vertical polarization fits well in the central peak, but shows deviations at the second peak near 176°. The optimum refractive index is 1.585 to 1.590, but again the second peak is disappointing. For $R = 5.055$ μm, Fig. 8(a) shows a good fit for horizontal polarization at the second and third peaks near 177.5° and 175°, but fails to fit the central peak (180°) because the data is too low, although the closest fit is with a refractive index of 1.580. Figure 8(b) for vertical polarization fits well everywhere for a refractive index of 1.585.

B. Backscattering from Water Droplets

Backscattering from water droplets produced from an atomizer is shown in Fig. 9 for both vertically and horizontally polarized incident light. The intensity is normalized at 178°. From previous light scattering work done in our laboratory, our water droplets had a weighted mean radius of 1.1 μm with a geometric width of 1.5 for a log-normal size distribution [16]. Using these parameters, the theoretical data were generated by the Laven MiePlot to compare with the experimental data. Overall, the experimental results fit fairly well with the Mie theory using the indisputable refractive index for water of 1.33 for angles of 180° ± 3°, but then deviations mount.

6. DISCUSSION AND CONCLUSIONS

The purposes of this paper was to study, apparently for the first time experimentally, the angular dependence of backscattering from spheres in the few-micron-size range and thereby demonstrate and make known the sensitivity of backscattering on the properties of the scattering spheres. We hope to condition the experimentalist with regard to the accuracy one can expect in a backscattering experiment. The situations displayed in Figs. 7–9, where the fits of the data to Mie theory were at times either good or not so good, are not a result of poor experimental procedure. Instead, the situations are due to the often extreme sensitivity of backscattering to the parameters of size, refractive index, and shape as demonstrated in the theoretical results in Figs. 4–6. These results will be important as we and others study backscattering from other particle shapes and use scattering from spheres as a calibration. These results also alert workers in fields such as particle metrology and LIDAR that interpretation of backscattered and near-backscattered light is very sensitive to the optical, size, and shape parameters of the scatterers.

Funding. National Science Foundation (NSF) (AGM 1261651); U.S. Army Research Laboratory (ARL) (W911NF-14-1-0352).

Acknowledgment. We thank Tim Sobering, Russell Taylor, and David Huddleston for the detector's electronic design. We are grateful to Russ Reynolds for his help on building and modifying our research instrumentation.

REFERENCES

1. M. Minnaert, *Light and Color in the Outdoors* (Springer-Verlag, 1974).
2. H. C. van de Hulst, *Light Scattering by Small Particles* (Dover, 1981).
3. H. N. Nussenzveig, "High-frequency scattering by a transparent sphere. II. Theory of the rainbow and the glory," J. Math. Phys. **10**, 125–176 (1969).
4. H. M. Nussenzveig, "Complex angular momentum theory of the rainbow and the glory," J. Opt. Soc. Am. **69**, 1068–1079 (1979).
5. H. M. Nussenzveig, "Does the glory have a simple explanation?" Opt. Lett. **27**, 1379–1381 (2002).
6. P. Laven, "How are glories formed?" Appl. Opt. **44**, 5675–5683 (2005).
7. T. S. Fahlen and H. C. Bryant, "Direct observation of surface waves on water droplets," J. Opt. Soc. Am. **56**, 1635–1636 (1966).
8. T. S. Fahlen and H. C. Bryant, "Optical back scattering from single water droplets," J. Opt. Soc. Am. **58**, 304–310 (1968).
9. M. J. Saunders, "Near-field backscattering measurements from a microscopic water droplet," J. Opt. Soc. Am. **60**, 1359–1365 (1970).
10. K. Sassen, "Optical backscattering from near-spherical water, ice, and mixed phase drops," Appl. Opt. **16**, 1332–1341 (1977).
11. B. Redding, Y.-L. Pan, C. Wang, and H. Cao, "Polarization-resolved near-backscattering of airborne aggregates composed of different primary particles," Opt. Lett. **39**, 4076–4079 (2014).
12. P. Laven, "Simulation of rainbows, coronas, and glories by use of Mie theory," Appl. Opt. **42**, 436–444 (2003).
13. K. Muinonen, E. Zubko, J. Tyynela, Y. G. Shkuratov, and G. Videen, "Introduction to light scattering by Gaussian random particles with discrete-dipole approximation," J. Quant. Spectrosc. Radiat. Transfer **106**, 360–377 (2007).
14. B. Draine and P. Flatau, "Discrete-dipole approximation for scattering calculations," J. Opt. Soc. Am. **11**, 1491–1499 (1994).
15. M. Yurkin and A. G. Hoekstra, "The discrete-dipole-approximation code ADDA: capabilities and known limitations," J. Quant. Spectrosc. Radiat. Transfer **112**, 2234–2247 (2011).
16. Y. Wang, A. Chakrabarti, and C. M. Sorensen, "A light-scattering study of the scattering matrix elements of Arizona road dust," J. Quant. Spectrosc. Radiat. Transfer **163**, 72–79 (2015).